STUDY OF A PIEZOELECTRIC ACCELEROMETER BASED ON D_{33} MODE

Hui ZHOU[1, 2], Rui-hua HAN[1], Ma-hui XU[1], Hang GUO[1, *]

[1]Pen-Tung Sah Institute of Micro-Nano Science and Technology, Xiamen University, Fujian, 361000, China
[2]College of Physical Science and Technology, Xiamen University, Fujian, 361000, China
[*]Corresponding author, E-mail: hangguo@xmu.edu.cn.

A piezoelectric accelerometer based on d_{33} mode was studied in this work. It is comprised of multiple cantilever beams to support a central seismic mass. The piezoelectric PZT thin films and interdigital (IDT) electrodes are designed to be deposited on the surface of beams. The PZT thin film was in-plane polarized and worked in d_{33} mode. The accelerometer was fundamentally analyzed and designed by using finite element method in ANSYS. Results showed that the presented micro piezoelectric accelerometer in d_{33} mode can offer higher voltage output over that in d_{31} mode, significantly improving the sensitivity without lowering the bandwidth.

Keywords: Piezoelectric accelerometer; MEMS; D_{33} mode; D_{31} mode; In-plane; IDT electrodes

1. INTRODUCTION

Accelerometers fabricated by the MEMS technology are in high demand for applications in aerospace, automobiles, military systems, and biomedical engineering fields. Various sensing mechanisms have been put forward in accelerometers, such as piezoresistive, capacitive and piezoelectric [1-4]. Generally, an external power source is required for the capacitive and piezoresistive accelerometers; whereas piezoelectric type accelerometers can directly detect the electrical signals generated by piezoelectric material, thus their operation could consume less energy and does not even necessarily require an external power supply. Besides, piezoelectric accelerometers showed better performance over the other two types of accelerometers in temperature stability and dynamic characteristics. Consequently, piezoelectric accelerometers draw an increasing attention in recent years.

Currently, piezoelectric accelerometers are mostly designed in a kind of cantilever structure with four cantilever beams supporting a central seismic mass. Electrodes and thin films of PZT or other piezoelectric materials were sequentially deposited on the suspended beams to form a *sandwich* structure. When the mass is subjected to an acceleration in the vertical direction, the cantilever beam structure will move vertically. The PZT thin films will deform along with the cantilever. As a result, charge can be generated on the PZT thin films due to piezoelectric effect, i.e., the piezoelectric coefficient d_{31} of the PZT thin film, and then detected by electrodes. However, the deformation in horizontal directions is generally very limited, resulting in an extremely low horizontal sensitivity. With d_{33} mode design, a kind of interdigital (IDT) electrode configuration was used in the piezoelectric accelerometer. The gap between two fingers of the IDT electrodes can reach up to 5-10μm that is equivalent to increasing thickness of the PZT film in the horizontal direction. Thus, a thicker PZT film and smaller capacitance of the configuration can lead to a higher horizontal sensitivity and a larger output voltage of the accelerometer. Hindrichsen at el used a screen printing method to deposit a 60μm thick PZT film on the cantilever beams with the horizontal voltage sensitivity up to 4.15mV/g [5]. Zou et al developed a bimorph cantilever beam with multilayer deposited on the beam, which effectively improved the horizontal sensitivity and mechanical properties of the beam as well [6].

In this work, a micro piezoelectric accelerometer working in d33 mode was studied, with a pair of IDT electrodes deposited on the PZT thin film to replace the conventional sandwich structure. As a consequence, the PZT thin films can be polarized along the in-plane direction. Reasons for such an in-plane polarization were outlined as follows: (1) The output voltage of PZT thin film is seriously restricted by the limited thickness obtained by the sputtering or Sol-Gel method; (2) The electrical output generated over the electrodes is determined by the longitudinal piezoelectric coefficient d_{33}, which is usually significantly larger than the transverse piezoelectric coefficient d_{31} utilized in the *sandwich* electrode configuration; (3) The fabrication and package processes become simpler without the need to use and connect the bottom electrode.

2. THEORETICAL ANALYSIS

2.1. Basic principle

As shown in Fig.1, when the mass was subjected to an

978-1-5090-1189-6/16/$31.00 ©2016 IEEE

inertia force in the vertical direction, it would move vertically. The PZT film would deform with the cantilever to generate charges in the film due to piezoelectric effect. The IDT electrodes on the surface of the PZT thin film could detect and collect these generated charges [7]. In order to improve the horizontal sensitivity and bandwidth, the accelerometer have several silicon-based composite beams suspended from the outer frame to a seismic mass located at the center of the acceleromter. As shown in Fig. 2, the top surface of each suspended beam was deposited with the PZT thin film and IDT electrodes.

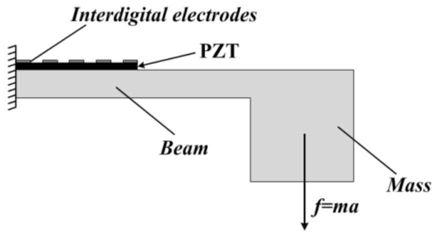

Figure 1 Principle of the micro piezoelectric accelerometer in d_{33} mode

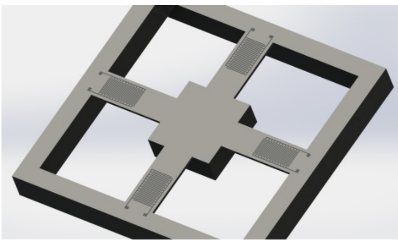

(a) Schematic diagram of micro piezoelectric accelerometer in d_{33} mode

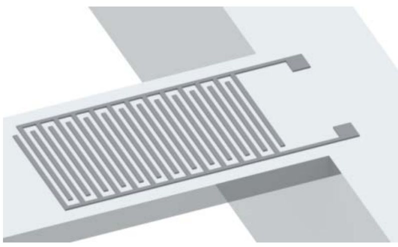

(b) Close view of IDT electrodes for d_{33} mode

Figure 2 Structural configuration of the micro piezoelectric accelerometer in d33 mode

2.2. Comparison of d_{33} and d_{31} modes

The d_{31} and d_{33} modes are generally two types of configurations of piezoelectric transduction applied in MEMS transducers. In Fig. 3(a), a vertical electrical field is created when a horizontal strain is applied in the film. Parallelized electric potential resulting from the electric field could be detected by the metallic electrodes. Fig. 3(b) shows a typical device in d_{33} mode, in which a set of ITD electrodes were used to measure charges generated by the in-plane horizontal strain. As noted in this figure, the direction of the polarization vector alternates between adjacent IDT cells.

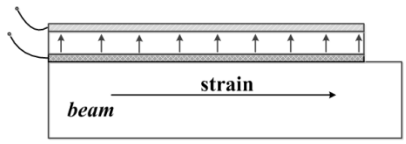

(a) In d_{31}mode: electrical field in vertical direction generated due to horizontal strain

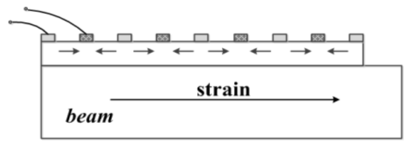

(b) In d_{33}mode: electrical field in horizontal direction generated due to horizontal strain

Figure 3 Comparison of two modes for piezoelectric transducers

2.3. Calculation of the capacitance and charge

As shown in Fig. 4(a), the full electrode set is comprised of many cells electrically connected in parallel. Analysis of the IDT electrode structure in d_{33} mode may be performed by analyzing a single unit cell. The analysis was based on these following assumptions: (1) Electric fields only exist in regions between electrodes; (2) Electric field are horizontal; (3) Electric fields are of constant magnitude through the thickness of the PZT films.

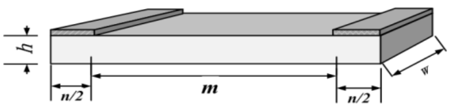

(a) Schematic diagram of a pair of electrode in d_{33} mode

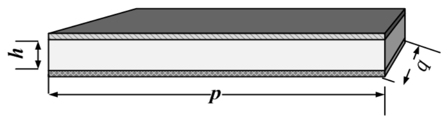

(b) Schematic diagram of electrodes in d_{31} mode

Figure 4 Structural configuration of electrodes in two modes

The fill factor η is defined as the volume ratio of active region to the full cell, which is

$$\eta = \frac{m}{m+n} \tag{1}$$

where *m* represents the volume of region between the electrodes with a distance of *m*, and *m*+*n* represents the volume of full cell with a distance of *m*+*n*.

The unit capacitance C_0 is defined as

$$C_0 = \frac{\varepsilon_0 \cdot \varepsilon_{33} \cdot w \cdot h}{m} \tag{2}$$

where ε_{33} is the effective dielectric constant, and *w* and *h* are the width and thickness of the beam, respectively. The electric displacement D_3 resulted from the strain S_3

is

$$D_3 = d_{33} \cdot S_3 \tag{3}$$

where d_{33} is the piezoelectric strain constant and S_3 is the strain along the X-axis. It is a function of the vertical displacement. According to force and moment balance conditions [8], the neutral surface of the cantilever is located at a, which is

$$a = \frac{1}{2}\frac{E_s h^2 - E_p h_{pzt}^2}{E_s h + E_p h_{pzt}} \tag{4}$$

where E_s and E_p are the Young's modulus of silicon and PZT thin films, respectively, and h is the thickness of the silicon beam and h_{pzt} is the thickness of the PZT thin film. The strain S_3 is derived as

$$S_3 = (E_p M(x) / EI_{eq})(h_{pzt} / 2 + a) \tag{5}$$

In order to simplify the expression of the formula, an equivalent formula was introduced, which is

$$\begin{aligned} EI_{eq} &= 1/3[wE_s(h^3 - 3h^2 a + 3ha^2)] + \\ &1/3[wE_p(h_{pzt}^3 + 3h_{pzt}^2 a + 3h_{pzt} a^2)] \end{aligned} \tag{6}$$

Thus, we can obtain

$$D_3 = d_{33}(E_p M(x) / EI_{eq})(h_{pzt} / 2 + a) \tag{7}$$

The charge generated by ambient vibration could be derived as

$$Q = \eta \cdot \int_0^{0.5l} D_3 w dx = \frac{\eta}{32} d_{33} w \frac{E_p}{EI_{ep}} (a + \frac{h_{pzt}}{2}) m_0 g a l^2 \tag{8}$$

where m_0 and g are the mass of the seismic mas block and the gravitational acceleration, respectively. The total capacitance can be expressed as

$$C = C_0 \cdot N = \varepsilon_0 \varepsilon_{33} \frac{h \cdot w}{m} \cdot \frac{0.5l}{m+n} \tag{9}$$

where N is the number of the unit cell, l the total length of the beam, and ε_0 the vacuum permittivity.

With respect to the d_{33} mode electrode configuration, capacitance and charge generated in a pair of IDT electrode in d_{31} mode can be calculated. As shown in Fig. 4(b), the electrodes and the PZT thin film can be treated as a parallel plate capacitor due to the insulation nature of PZT. When it is subjected to an external force, positive and negative charges are uniformly distributed on the surface of the PZT thin film.

The capacitance of a parallel plate capacitor C is

$$C = \frac{\varepsilon_0 \cdot \varepsilon_{33} \cdot p \cdot q}{h} \tag{10}$$

where ε_{33} is the relative dielectric constant of the PZT thin film, $p \cdot q$ and h are the area of the electrodes and the distance between them, respectively. The charges generated during the movement may be calculated as

$$Q = C \cdot V \tag{11}$$

With the formulas derived above, we can analyze and design the micro piezoelectric accelerometer in d_{33} mode. In order to explore the relationship between the charge sensitivity and the beam structures, the initial values of the geometric size and materials properties should be given out.

The thickness of the cantilever beam and the PZT thin film is largely limited by the experimental conditions and the preparation processes. The thickness of the cantilever beam and the PZT thin films was initially set as 55 and 1.2μm, respectively. The charge sensitivity of the accelerometer is mainly affected by the length of the cantilever beam. Here, the length and width of the cantilever beam were set in the range of 500μm to 2500 μm and 100μm to 500μm, respectively, and beam width was set as 500μm. The piezoelectric constant d_{33} was set as 168pC/N[4], and other parameters about material properties are listed in Table I.

Table I Materials properties

Constant	value
d_{33} (Pc/N)	168 [4]
Es (Gpa)	142.5 [4]
Ep (Gpa)	70.2 [4]
ε_{33}	1475(ε_0) [4]

As can be seen in Fig. 5, with the increase of the beam length, the charge sensitivity experience a gradual rise. As for the width of the beam, it can be concluded from the above derived equations (6) and (8) that the width has no effect on the charge sensitivity. This indicates that the design of the accelerometer should increase the length of the cantilever to increase the charge sensitivity of the accelerometer. But, it will also affect the resonance frequency, i.e. the bandwidth of the micro piezoelectric accelerometer.

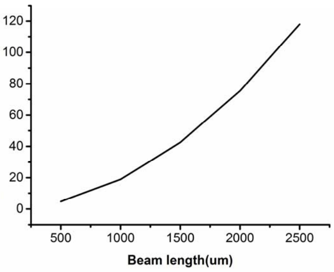

Figure 5 The effect of beam length on charge sensitivity

As for the size of the ITD electrodes, it is mainly affected by the microfabrication conditions. In this work, the fill factor η and the gap between the ITD electrodes were set as 0.5 and 5 μm, respectively [9].

3. FINITE ELEMENT ANALYSIS

3.1. Strain distribution

Finite element analysis in ANSYS are conducted for evaluation of performance of the micro piezoelectric accelerometer.

The strain contour was studied with the acceleration input in the out-of-plane direction, as shown in Fig. 6. It helps to identify the regions where the maximum and minimum stress and strain lies. To avoid the fracture at the joints caused by very high acceleration, the silicon beams were connected perpendicularly to the edges of the supporting frame. The IDT electrodes were positioned based on the strain contour from the simulation result. As shown in Fig. 6, with the out-of-plane acceleration applied, the strain gets the maximum value at the two ends of the silicon composite beams but in opposite direction, with a neutral line around the center of the beams. In order to constructively collect the electrical output in response to the acceleration, the IDT electrodes were placed only near one end of the silicon composite beam, where the strain is in the same direction.

3.2. Charge distribution

Voltage or charge sensitivity refers to the voltage or charge produced by the accelerometer under unit acceleration. Under normal circumstance, a higher voltage or charge sensitivity for simple subsequent signal detection and analysis is always preferred.

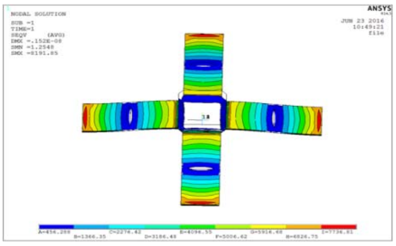

Figure 6. Strian distribution in d33 mode

In order to compare the voltage sensitivity of two different working modes, the two accelerometers were designed with the same structure configuration. The only difference is the direction of polarization of the piezoelectric material. Namely, the polarization direction of piezoelectric material under d_{33} mode is horizontal, while vertical for d_{31} mode.

From the voltage contour (See Fig. 7(a)), it is clearly that the voltage on the PZT films presents symmetrical distribution when it was subjected to a vertical acceleration, descending from the seismic mass to support frame. This result implies that the acceleration in vertical direction can be detected. The voltage sensitivity can be calculated to be 4.55 mV/g, which is much higher than 0.012 mV/g of voltage sensitivity in d_{31} mode. When the accelerometer is subjected to a horizontal acceleration, X-axis for example, the seismic mass will rotate around Y-axis and produce tensile and compressive stress anti-symmetrically distributed on the two beams along X-axis. As shown in Fig. 8(b), the voltage in Y-axis is almost zero due to limited deformation, which can be neglected compared with the voltage in X-axis. The acceleration in horizontal can also be detected. Compared to the micro accelerometer in d_{31} mode, the voltage sensitivity improved from 0.185mV/g to 0.497 mV/g.

3.3. Resonant frequency

The resonant frequency is a natural attribute of the object. It is only related to the structure of the object, rather than to the state of motion or external load. The bandwidth or operation range of an accelerometer is limited by the 1st order resonant frequency, i.e the fundamental frequency. The structure would be destroyed once the loaded frequency is very close to exceeds the resonant frequency in a short range. It is believed that two different modes should have similar resonant frequency due to the same structure. Simulation results showed that resonant frequencies at the same size of the structures for both d_{33} and d_{31} modes were 13485Hz and 13340Hz, respectively, which are very close to each other.

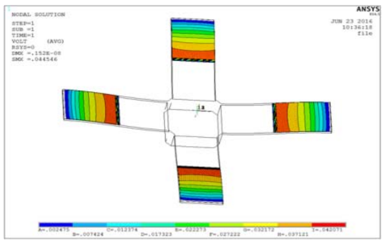

(a) charge distribution under vertical acceleration in d_{33} mode

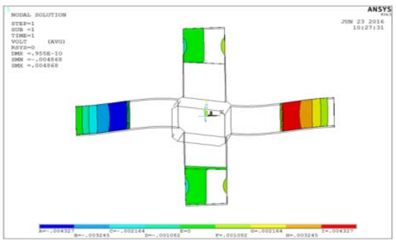

(b) charge distribution under horizontal acceleration in d_{33} mode

Figure 7 Charge distribution of the micro piezoelectric accelerometer in d33 mode

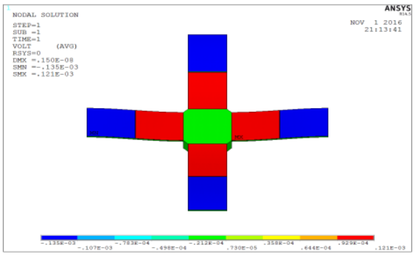

(a) Charge distribution under vertical acceleration in d_{31} mode

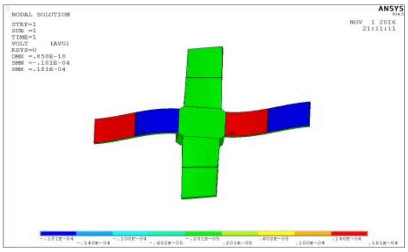

(b) charge distribution under horizontal acceleration in d_{31} mode

Figure 8 Charge distribution of the micro piezoelectric accelerometer in d33 mode

4. CONCLUSIONS

In this work, a piezoelectric accelerometer with significantly improved voltage sensitivity was obtained by selection of a d_{33} working mode. Results showed that both the vertical and horizontal sensitivity could be effectively enhanced with this design. The vertical and voltage horizontal sensitivity increased from 0.012V/g to 4.55mV/g and 0.185mV/g to 0.497mV/g, respectively. Manufacturing process could be simplified at the same time. Furthermore, bandwidth and mechanical strength were guaranteed since the design almost did not change the structure of the micro piezoelectric accelerometer.

ACKNOWLEDGMENT

This work is financially supported by the Scientific Research and Development Program of City of Xiamen (3502Z20143003) and the Collaboration between Industry and University Program of Fujian Province (2015H6021).

REFERENCES

[1] Partridge A, Reynolds JK, et al. A high-performance planar piezoresistive accelerometer. *Journal of microelectromechanical systems*, 9(1):58-66, 2000.

[2] Chae J, Kulah H, Najafi K. A monolithic three-axis micro-g micromachined silicon capacitive accelerometer. *Journal of microelectromechanical systems*, 14(2):235-242, 2005.

[3] Selvakumar A, Najafa K. A high-sensitivity z-axis capacitive silicon microaccelerometer with a torsional suspension. *Journal of Microelectromechanical Systems*, 7(2):192-200, 1998.

[4] Shen ZY, Tan CY, Yao K, Zhang L, Chen YF. A miniaturized wireless accelerometer with micromachined piezoelectric sensing elements. *Sensors and Actuators A:Physical*, 241:313-319,2016.

[5] Hindrichsen CC, Almind NS, Broderson SH, et al. Analytical model of a PZT thick-film triaxial accelerometer for optimum design. *IEEE Sensors Journal,* 9(4):419-429, 2009.

[6] Hindrichsen CC, Thomsen EV. MEMS Accelerometer with Screen Printed Piezoelectric Thick Film. *In Proc.5th IEEE Conf. Sensors, pp. 1477-1488,* 2004.

[7] Zou Q, Kim ES. Single and triaxis piezoelectric-bimorph accelerometers. *Journal of Microelectro-mechanical Systems*, 17(1):45-57, 2008.

[8] Hillenbrand J, Kodejska M, Sessler GM, et al. High-sensitivity piezoelectret-film accelerometers. *IEEE Transactions on Dielectrics and Electrical Insulation*, 17(4):1021-1027, 2010.

[9] Wang QM, Yang ZC, Li F, et al. Analysis of thin film piezoelectric microaccelerometer using analytical and finite element modeling. *Sensors and Actuators A: Physical*, 113(1):1-11, 2004.

[10] Kim D, Hewa-Kasakarage NN, Hall NA. A theoretical and experimental comparison of 3-3 and 3-1 mode piezoelectric microelectromechanical systems (MEMS). *Sensors and actuators A: physical*, 134(5):112-122, 2013.